Research Article | Vol. 33, No. 17 / 25 Aug 2025 / Optics Express 37017
Optics EXPRESS

Bi-tone-driven optomechanical photon blockade

YUWEI JING,[1] JIAN TANG,[2] YUNLAN ZUO,[3] BAIJUN LI,[4] AND KEYU XIA[1,*]

[1]College of Engineering and Applied Sciences, National Laboratory of Solid State Microstructures, and Collaborative Innovation Center of Advanced Microstructures, Nanjing University, Nanjing 210023, China
[2]Department of Physics and Synergetic Innovation Center for Quantum Effects and Applications, Hunan Normal University, Changsha 410081, China
[3]School of Physics and Chemistry, Hunan First Normal University, Changsha 410205, China
[4]Institute of Quantum Precision Measurement, State Key Laboratory of Radio Frequency Heterogeneous Integration, College of Physics and Optoelectronic Engineering, Shenzhen University, Shenzhen 518060, China
*keyu.xia@nju.edu.cn

Abstract: Optomechanical systems are capable of coupling to various engineered quantum systems. The ability of extending optomechanical systems to the quantum regime holds the potential for wide applications in quantum information processing and quantum sensing. Due to its importance in single-photon sources and hybrid quantum devices, optomechanical photon blockade (OMPB) has been theoretically predicted with various types of interactions. However, the realization of OMPB requires strict conditions, such as strong optomechanical coupling or precise control of system parameters. Here, we propose how to release such conditions and realize OMPB with experimentally accessible parameters. We find strong OMPB in a weak coupling regime by using bi-tone drive. Moreover, such OMPB can be flexibly controlled by tuning optical detuning. Our work provides a method for achieving strong antibunched photon-photon correlation in weak coupling optomechanics, enabling hybrid quantum devices for applications in quantum information processing.

1. Introduction

Optomechanical systems (OMSs), featuring the interaction of electromagnetic radiation with the motion of mechanical objects, have been recognized as a powerful platform for modern science and technology [1,2]. In optical information processing, OMSs have been proposed as a novel technology for optical memory [3] and single-photon detection [4]. These versatile systems have been shown to serve as key elements of nonreciprocal transport of photons and phonons [5–8], such as optomechanical isolators [9,10] or circulators [11]. Moreover, OMSs also enable various sensing applications, ranging from magnetometry [12], displacement [13] and acceleration [14] sensors, to the measurement of weak-force [15–18] and gravitational-wave [19,20] combined with squeezed light. In addition, intriguing optomechanical effects, including normal-mode splitting [21–24], phonon lasing [25–34], and optomechanically induced transparency [35–42], have been explored based on OMSs, and even with non-Hermitian [29–31,38–41,43–45] or topological OMSs [46–50].

Once an OMS is cooled to the quantum ground state [51–54], it provides a powerful platform to process quantum information. Beyond traditional laser optics and classical physics, which focus on controlling or measuring classical quantities, recent developments of OMSs have also shown their potentials in quantum information technologies [55,56], such as quantum transduction [57,58], preparation of squeezed states [59–61], as well as the creation of entanglement and non-classical correlations [51,62–68]. Other quantum effects, including dynamical Casimir effect [69] and optomechanical quantum phase transitions [70] have also been studied in OMSs. Particularly, optomechanical photon blockade (OMPB), a typical quantum effect, has been

#568384 https://doi.org/10.1364/OE.568384
Journal © 2025 Received 20 Jun 2025; revised 30 Jul 2025; accepted 31 Jul 2025; published 21 Aug 2025

Optics EXPRESS

explored in linear [71] or quadratic [72] OMSs, due to its potential applications for creating or controlling non-classical light and realizing novel quantum devices [73–76]. Such conventional OMPB requires strong optomechanical coupling, i.e., the single-photon optomechanical coupling strength is larger than optical dissipation rate ($g_0 > \kappa$), resulting in unequal eigenenergy spaces. Therefore, a monochromatic drive is only resonant for the transition from the vacuum to the one-photon state, but not for higher transitions. However, such strong optomechanical interaction at the single-photon level is challenging for achieving in realistic OMSs.

Several methods for realizing conventional OMPB have been theoretically proposed by introducing hybrid electro-optomechanical system [77], squeezed light [78], parametric mechanical driving [79], or additional cross-Kerr nonlinearity [80] to enhance optomechanical interactions. The poineering study of unconventional photon blockade [81–83] release the condition of strong single-photon nonlinearities [84,85], showing that photon blockade can be realized in the weak-nonlinearity regime. However, these strategies require not only an additional optical mode but also fine tuning of system parameters. Till now, OMPB has not been experimentally demonstrated yet.

Here, we propose how to realize OMPB in the weak coupling regime by tuning the input lasers without precise control of system parameters. Specifically, we found a near-perfect dynamical OMPB effect with $g^{(2)}(t) \sim 0.01$ for $g_0/\omega_m = 0.05$ induced by two coherent drives with different frequencies. This effect can be understood from the destructive quantum interference between different transition paths from the vacuum to the two-photon state via bi-tone drives, leading to the cancellation of the two-photon population. While photon blockade is typically detected with the equal-time second order correlation function $g^2(0) < 1$ [82–85], the time-dependent nature of the system steady-state can induce periodicity antibunching at special time window, resembling that in pulse-driven dynamical photon blockade [86]. The bi-tone driving scheme further introduces an additional degree of freedom, e.g., the photon frequency, enabling near-perfect photon blockade to be achieved simply by tuning the frequency and amplitude of the applied radio-frequency drive. Compared to unconventional photon blockade [84,85], which demands precise tuning of cavity resonances and coupling strengths, this method is more experimentally accessible.

We note that this mechanism has previously been used to study single-mode photon blockade with purely optical nonlinearities [87–89], showing that single and two windows of photon blockade can solely exist in the single- and two-mode optical systems, respectively. In contrast, both of the single and two windows of OMPB can be realized in this bi-tone-driven OMS, and can be switched by tuning the driving detuning. This provides better flexibility in controlling OMPB at the single-photon level.

Our work opens up a new route for realizing dynamical OMPB with experimentally accessible conditions for current optomechanical platforms, enabling novel quantum devices, such as optomechanical switch of single photons or optomechanical single-photon source.

2. Bi-tone-driven optomechanics

We consider an OMS driven by a bi-tone laser composed of a continuous-wave laser at frequency ω_p and a sideband laser at frequency ω_s, as shown in Fig. 1(a). The system can be described by the Hamiltonian ($\hbar = 1$),

$$\begin{aligned} H_{\rm sys} &= H_{\rm opt} + H_{\rm dri} \\ H_{\rm opt} &= \omega_c a^\dagger a + \omega_m b^\dagger b + g_0 a^\dagger a \left(b^\dagger + b\right) \\ H_{\rm dri} &= \epsilon_p \left(a^\dagger e^{-i\omega_p t} + a e^{i\omega_p t}\right) + \epsilon_s \left(a^\dagger e^{-i\omega_s t} + a e^{i\omega_s t}\right), \end{aligned} \tag{1}$$

with resonant frequency ω_c of cavity and frequency ω_m of mechanical mode. Here, $\hat{a}$ ($\hat{b}$) is the annihilation operator for the optical (mechanical) mode, g_0 is the single-photon optomechanical

Optics EXPRESS

coupling strength, and ϵ_p (ϵ_s) is the driving field with frequency of ω_p (ω_s). To diagonalize the Hamiltonian, we introduce the following unitary operator:

$$D(\beta_0) = e^{\beta_0 a^\dagger a\left(b^\dagger - b\right)}, \tag{2}$$

with $\beta_0 = -g_0/\omega_m$. It is easy to make a unitary transformation on the Hamiltonian of the cavity OMS:

$$\widetilde{H}_{\text{opt}} = D^\dagger H_{\text{opt}} D = \omega_c a^\dagger a + \omega_m b^\dagger b - \delta\left(a^\dagger a\right)^2, \tag{3}$$

where $\delta = g_0^2/\omega_m$. To eliminate the linear/non-diagonal term, we assume $\omega_m\beta_0 + g_0 = 0$. Then, we can easily obtain the eigenstates and eigenvalues of diagonal Hamiltonian via unitary operator:

$$\widetilde{H}_{\text{opt}} |m\rangle_a |l\rangle_b = E_{m,l} |m\rangle_a |l\rangle_b . \tag{4}$$

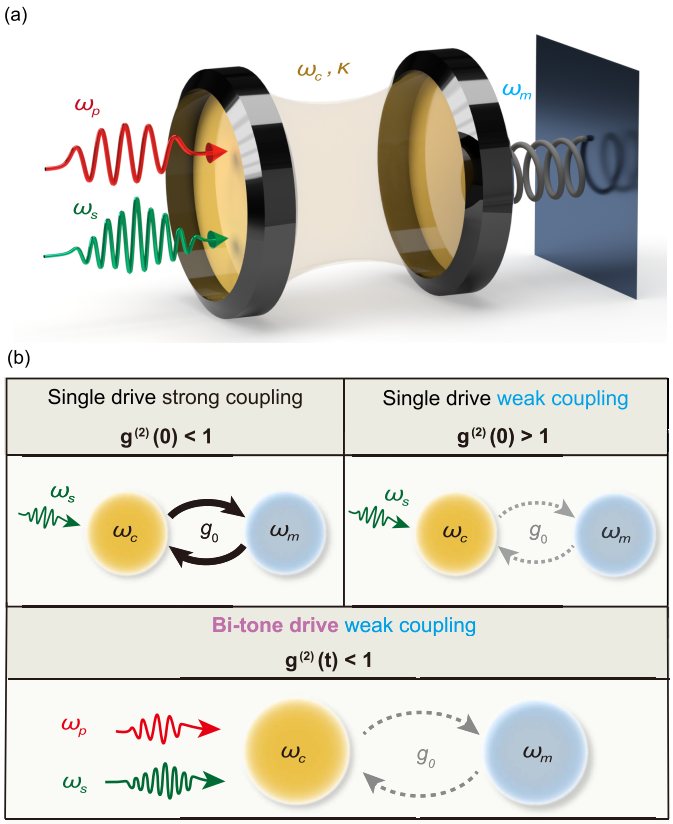

Fig. 1. (a) Schematic diagram of system. A driving field with frequency ω_p and a detuned laser field with frequency ω_s are injected into the weakly coupled optomechanical cavity. Here, ω_c (ω_m) denotes the resonant frequency of the cavity field (mechanical oscillation), and κ represents the optical dissipation rate. (b) A comparison between a single-drive strong coupling OMS, a weak coupling OMS, and a bi-tone drive weak coupling OMS.

Here, we use $|m\rangle_a$ and $|l\rangle_b$ $(m, n = 0, 1, 2, \ldots)$ to represent the Fock states of the cavity field and the mechanical oscillator, respectively. Specifically, $|l(m)\rangle_b$ denotes the displacement states

Optics EXPRESS

of $|l\rangle_b$. Therefore, the eigenvalues of the system Hamiltonian can be expressed as:

$$E_{m,l} = m\omega_c + l\omega_m - m^2\delta. \tag{5}$$

In the frame rotating with the driving frequency ω_p, the effective Hamiltonian of the system can be written as:

$$\begin{aligned} H_{\mathrm{r}} =& \Delta_c a^\dagger a + \omega_m b^\dagger b + g_0 a^\dagger a \left(b^\dagger + b\right) + \epsilon_1 \left(a^\dagger + a\right) \\ &+ \epsilon_2 \left(a^\dagger e^{-i\Delta_s t} + a e^{i\Delta_s t}\right), \end{aligned} \tag{6}$$

with $\Delta_c = \omega_c - \omega_p = -\delta$ (single-photon resonance) and $\Delta_s = \omega_s - \omega_p$. Due to the completeness of the eigenstates, the bi-tone optical field can excite photons in the ground state through different paths under a very weak driving strength, ϵ_p (ϵ_s) $\ll \kappa$ (where κ is the optical dissipation rate). Consequently, the excitation of higher photon number states can be neglected in the weak driven case, and the system can be confined to the zero-, one-, and two-photon subspaces. The system Hamiltonian can thus be expressed in the spectral representation as:

$$\begin{aligned} H_{\mathrm{r}} =& \sum_{m=0}^{2} \sum_{l=0}^{\infty} \sum_{l'=0}^{\infty} \Delta_{m,l} |m\rangle_a |l\rangle_b \langle m|_a \langle l|_b \\ &+ E\sqrt{m+1} \langle \widetilde{l}(m+1)|l'(m)\rangle_b |m+1\rangle_a |\widetilde{l}(m+1)\rangle_b \langle m|_a \langle l'(m)|_b \\ &+ E^*\sqrt{m+1} \langle \widetilde{l}(m)|\widetilde{l}(m+1)\rangle_b |m\rangle_a |\widetilde{l}(m)\rangle_b \langle m+1|_a \langle \widetilde{l}(m+1)|_b, \end{aligned} \tag{7}$$

where $\Delta_{m,l} = m\Delta_c + l\omega_m - m^2\delta$, $E = \epsilon_p + \epsilon_s e^{-i\Delta_s t}$ and $|\widetilde{l}(m)\rangle_b = e^{m\beta_0(b^\dagger - b)}|l\rangle_b$. To evaluate photon blockade effects, it is essential to precisely control the intensity and phase of two coherent driving fields to specific parameters. We investigate the dynamics described by the two-photon equations of motion to determine the optimal pulse conditions for achieving photon blockade.

Now, we consider the total effective Hamiltonian including the damping term:

$$H_{\mathrm{eff}} = H_{\mathrm{r}} - \frac{i}{2}\kappa a^\dagger a - \frac{i}{2}\gamma_m b^\dagger b. \tag{8}$$

Here, the effect of quantum jumps is ignored in the semiclassical analytical approach. However, they are fully taken into account in the subsequent analysis based on the quantum master equation approach.

Under the weak excitation condition for both input fields $\epsilon_{p,s} \ll \kappa$, we investigate the system operating across multiple photon subspaces with ground states $|0\rangle$, $|1\rangle$ and $|2\rangle$. The general state of the system within this subspace can be expressed as:

$$|\phi(t)\rangle = \sum_{m=0}^{3} \sum_{l=0}^{\infty} C_{m,l} |m\rangle_a |l\rangle_b, \tag{9}$$

where $C_{m,l}$ are the probability amplitudes. In terms of the Eq. (8) and Schrödinger equation $i|\dot{\phi}(t)\rangle = H_{\mathrm{eff}}|\phi(t)\rangle$, by applying perturbation approximations to the Eq. (9), we compare the coefficients of the ground state and obtain the equations of motion for the probability amplitudes:

$$\begin{aligned} \dot{C}_{0,l}(t) =& -i\Delta_{0,l} C_{0,l}(t) \\ \dot{C}_{1,l}(t) =& -iAC_{1,l}(t) - i\sum_{k=0}^{\infty} EC_{0,k}(t) \langle \widetilde{l}(1)|k\rangle_b \\ \dot{C}_{2,l}(t) =& -iBC_{2,l}(t) - i\sqrt{2}\sum_{k=0}^{\infty} EC_{1,k} \langle \widetilde{l}(2)|\widetilde{k}(1)\rangle_b, \end{aligned} \tag{10}$$

with $A = \Delta_{1,l} - \frac{i}{2}\kappa - \frac{i}{2}\gamma_m$ and $B = \Delta_{2,l} - i\kappa - i\gamma_m$. Moreover, in the following condition of the destructive interference, γ_m is only included in the coefficients A and B. In addition,

Optics EXPRESS

the mechanical damping rate γ_m also meets the conditions of $\gamma_m \ll g_0$ ($\kappa \sim 0.05\omega_m$) and $\gamma_m \ll \epsilon$ ($\epsilon \sim 0.01\omega_m$). Therefore, the mechanical damping γ_m can be safely neglected in the conditions of destructive interference [72,90] . As an initial condition, we assume that there are no photons in cavity at the beginning, the solution for zero-photon amplitude can be written as:

$$C_{0,l}(t) = C_{0,l}(0)\, e^{-i\Delta_{0,l}t}. \tag{11}$$

We substitute it into the equation for the single-photon amplitude in Eq. (10) and introduce slowly-varying amplitude $C_{1,l}(t) = c_{1,l}(t)e^{-iAt}$ and $C_{1,l}(0) = c_{1,l}(0)$. The solution for the single-photon amplitude can be obtained by comparing the coefficients of the basis states:

$$\begin{aligned} C_{1,l}(t) = &-i\epsilon_p \sum_{k=0}^{\infty} \frac{\langle \widetilde{l}(1)|k\rangle_b C_{0,k}(0)}{i(A-\Delta_{0,k})}\left[e^{-i\Delta_{0,k}t} - e^{-iAt}\right] \\ &- i\epsilon_s \sum_{k=0}^{\infty} \frac{\langle \widetilde{l}(1)|k\rangle_b C_{0,k}(0)}{i(A-\Delta_{0,k}-\Delta_s)}\left[e^{-i(\Delta_{0,k}+\Delta_s)t} - e^{-iAt}\right], \end{aligned} \tag{12}$$

where $C_{0,l}(0)$ and $C_{0,k}(0)$ are determined by the initial state of oscillating mirror. Then the same method can be used to solve the two photon amplitude. By introducing varying amplitude $C_{2,l}(t) = c_{1,l}(t)e^{-i(\Delta_{2,l}-i\kappa)t}$ and dropping the higher-order [e.g. the second term of Eq. (12)], the solution for the two-photon amplitude in Eq. (10) is:

$$\begin{aligned} C_{2,l}(t) = &\sqrt{2}\epsilon_p^2 \frac{\langle \widetilde{l}(1)|0\rangle_b \langle \widetilde{l}(2)|\widetilde{k}(1)\rangle_b}{AB} \\ &+ \sqrt{2}\epsilon_p\epsilon_s \frac{\langle \widetilde{l}(1)|0\rangle_b \langle \widetilde{l}(2)|\widetilde{k}(1)\rangle_b}{(B-\Delta_s)}\left[\frac{1}{(A-\Delta_s)} + \frac{1}{A}\right]e^{-i\Delta_s t} \\ &+ \sqrt{2}\epsilon_s^2 \frac{\langle \widetilde{l}(1)|0\rangle_b \langle \widetilde{l}(2)|\widetilde{k}(1)\rangle_b}{(A-\Delta_s)(B-2\Delta_s)} e^{-2i\Delta_s t}, \end{aligned} \tag{13}$$

which can be ultimately written as a quadratic equation form of $\frac{\epsilon_s}{\epsilon_p}e^{-i\Delta_s t}$, that is:

$$C_{2,l}(t) = x_{pp} + x_{sp}\frac{\epsilon_s}{\epsilon_p}e^{-i\Delta_s t} + x_{ss}\frac{\epsilon_s^2}{\epsilon_p^2}e^{-2i\Delta_s t}, \tag{14}$$

where

$$\begin{aligned} x_{pp} &= \frac{\sqrt{2}\epsilon_p^2(\delta_{l,0} - \beta_0\delta_{l,1})^2}{AB} \\ x_{sp} &= \frac{\sqrt{2}\epsilon_p^2(\delta_{l,0} - \beta_0\delta_{l,1})^2}{(B-\Delta_s)}\left[\frac{1}{(A-\Delta_s)} + \frac{1}{A}\right] \\ x_{ss} &= \frac{\sqrt{2}\epsilon_p^2(\delta_{l,0} - \beta_0\delta_{l,1})^2}{(A-\Delta_s)(B-2\Delta_s)}, \end{aligned} \tag{15}$$

are the probability amplitudes generated by different driving fields, where $\delta_{l,n}$ is Dirac delta function. The probability amplitude of two-photon is evidently influenced by factors such as laser amplitude, driving frequency, and cavity dissipation. When $C_{2,l}(t) = 0$, destructive interference occurs among the various amplitude components, thereby impeding photon transitions to the Fock state $|2\rangle$. Consequently, the optimal ratio of two driven strengths can be obtained:

$$\left|\frac{\epsilon_s}{\epsilon_p}\right| = \left|\frac{-x_{sp} \pm \sqrt{x_{sp}^2 - 4x_{pp}x_{ss}}}{2x_{ss}}\right|. \tag{16}$$

Optics EXPRESS

3. Photon blockade with weak coupling

Furthermore, we can investigate the dynamical blockade of the system by numerically solving the time-dependent master equation. By introducing the density matrix of the cavity field $\rho(t)$ and Lindblad superoperator $D[O](\rho) = [O, \rho] = 2O\rho O^\dagger - OO^\dagger\rho - \rho O^\dagger O$, where $O = a, b$, the quantum master equation of the system can thus be expressed in the following form [91]:

$$L = -i[H, \rho] + \frac{\kappa}{2}D[a] + \frac{\gamma_m(n_{\rm th}+1)}{2}D[b] + \frac{\gamma_m n_{\rm th}}{2}D[b^\dagger], \tag{17}$$

where $n_{\rm th} = [\exp((\hbar\omega/(k_b{\rm T})) - 1)]^{-1}$ is the mean thermal phonon number of the mechanical mode at temperature T, with the Boltzmann constant k_b. The photon blockade is evaluated by the equal-time second-order quantum correlation function:

$$g^2(t) = \frac{\langle a^\dagger(t)a^\dagger(t)a(t)a(t)\rangle}{\langle a^\dagger(t)a(t)\rangle^2}. \tag{18}$$

Other weak-coupling photon blockade proposals [81–85,92,93], involving auxiliary cavity modes or parametric amplifiers, typically require precise tuning of intrinsic parameters of systems, such as cavity resonances and coupling strengths. In contrast, our method relies only on an additional driving tone. By simply adjusting the frequency and amplitude of the applied bi-tone drive, strong photon blockade can be achieved without the need for resonance or coupling matching.

In this study, we use the bi-tone scheme to achieve periodic modulation of different excitation fields, which makes the system alternate between photon bunching and antibunching. Figure 2(a) shows occurence of dynamical blockade for a weak optomechanical coupling strength (g/κ<1) by setting the optimal condition of ϵ_s/ϵ_p according to Eq. (16). We observe that for most of the time, the second-order correlation function $g^{(2)}(t)$ is near 1, indicating the weak anharmonicity caused by weak optomechanical coupling in the system. However, at certain specific moments, we find sharp oscillations in the second-order correlation function, exhibiting sub-Poissonian ($g^{(2)}(t)$<1) and super-Poissonian ($g^{(2)}(t)$>1) photon distributions. These drastic changes are consistent with our previous analysis, as destructive interference between different transition amplitudes leads to the suppression of the two-photon probability, as shown in Fig. 2(b) and (c). This phenomenon is entirely unobservable in traditional single-drive weak optomechanical coupling systems. Furthermore, we discover that within a single sharp oscillation period, two windows of photon blockade appear (i.e., $\kappa t_2/\omega_m = 90.07$ and $\kappa t_4/\omega_m = 91.07$). By controlling the phase delay of the driving field, sub-Poisson light can be selected from the coherent laser background [87]. To investigate this situation, we analyze the amplitude of each transition path considering the driving intensity, as follows:

$$T_{pp} = x_{pp}, \quad T_{sp} = x_{sp}\frac{\epsilon_s}{\epsilon_p}e^{-i\Delta_s t}, \quad T_{ss} = x_{ss}\frac{\epsilon_s^2}{\epsilon_p^2}e^{-2i\Delta_s t}. \tag{19}$$

As indicated by the red and green arrows in Fig. 2(c), the bi-tone drive excite the photons via different paths T_{pp}, T_{sp} and T_{ss}. The transition amplitudes of different paths induced by bi-tone drive are inhomogeneous, due to the phase detuning of the bi-tone input. Therefore, the destructive interference of these three amplitudes leads to the occurrence of dynamical blockade. Through our calculations, we find that for $\Delta_s/\omega_m = 0.15$, $|T_{sp}| < |T_{ss}| + |T_{pp}|$. Thus, when plotting the transition amplitudes in polar coordinates over different times and paths, we observe that blockade windows appear at two instantaneous points [Fig. 2(d)]. The expression for this is given

Optics EXPRESS

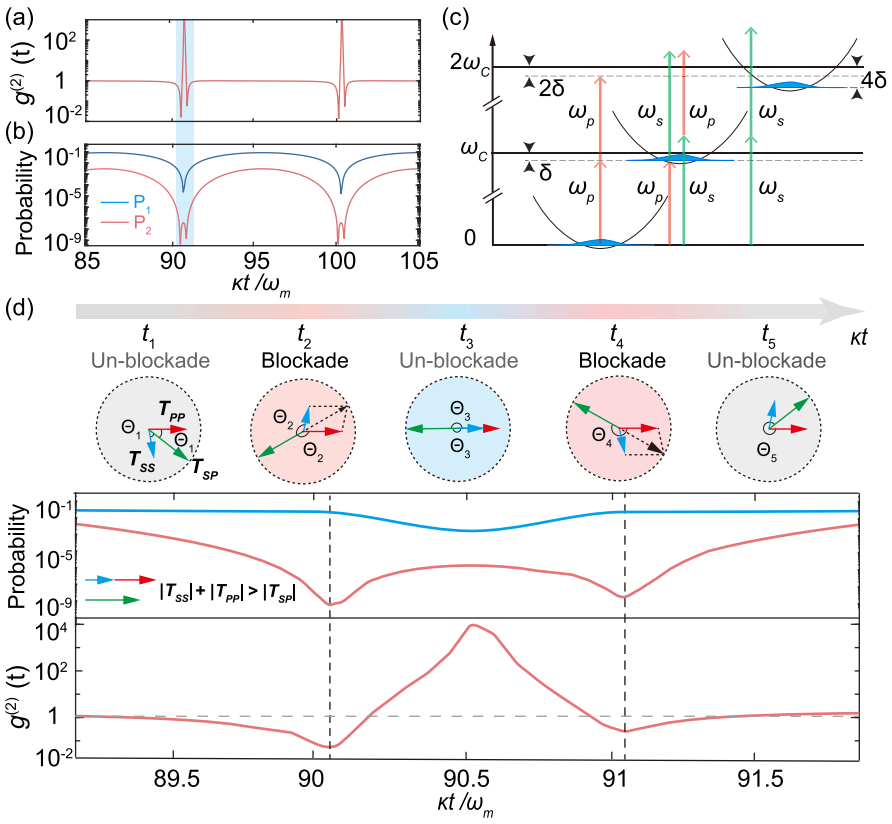

Fig. 2. The OMPB under the bi-tone driving field. (a) The equal-time second-order quantum correlation function $g^{(2)}(t)$ versus $\kappa t/\omega_m$ at optimal instants. The result shows two blockade windows within a single cycle period. (b) Populations P_1 and P_2 of Fock states $|1,0\rangle$ and $|2,0\rangle$, respectively. (c) Energy levels of a bi-tone driven OMS. Here $\delta = \omega_c - \omega_p = g_0^2/\omega_m, \Delta_s/\omega_m = (\omega_s - \omega_p)/\omega_m$. The underlying physics of this bi-tone OMPB can be understood from (d) the diagrams of probability amplitudes for different pathways in polar coordinate spaces at different times and the populations of Fock states. Here, the phase angle is defined as $\Theta_j = \theta + \Delta_s \cdot t_j$ for $j = 1, 2, 3, \ldots$. The parameter T_{ss} is independent of time, and ther parameters are taken as $g_0/\omega_m = 0.05$, $\Delta_s/\omega_m = 0.1$, $\kappa/\omega_m = 0.15$, $\gamma_m/\omega_m = 0.001$.

by:

$$t_s = \frac{2m\pi + \arg\left(\epsilon_s/\epsilon_p\right) - \arg(\varepsilon)}{\Delta_s}, \tag{20}$$

where ε denoting the term inside the vertical bar on the right side of Eq. (16). The first term indicates a periodic appearance of dynamical photon blockade. The second term is the external phase of the sideband laser, and the third term is due to the anharmonic response of the nonlinear cavity. In Fig. 2(a), we find that the finite time resolution used in evaluting $g^{(2)}(t)$ affects the difference between the values of the two windows t_2 and t_4. In fact, photon blockade can be characterized by the condition of $g^{(2)}$<0.5 in vaiours experiments: for example, $g^{(2)} \sim 0.45$ in atom-cavity system [94], $g^{(2)} \sim 0.38$ in WGM (Whispering Gallery Mode) cavity system [95], and $g^{(2)} \sim 0.3$ in cavity-free system [96]. Here, in our work both of the $g^{(2)}(t)$ of the two windows are much smaller than 0.5 [i.e., $g^{(2)}(t)$<0.1]. Therefore, the photon blockade effect of the two windows are efficient under the available experimental conditions.

Optics EXPRESS

More interestingly, we have discovered a switch from two blockade windows to a single blockade window within one period by adjusting the detuning between the two drives, as shown in Fig. 3(a) and (b). According to Eq. (15), the transition amplitude depends on the detuning and the optimal intensity ratio between the two input drives. By tuning the detuning, not only can the blockade period be regulated, but also the two windows within each period can be converted into a single window. For instance, when $\Delta_s/\omega_m = 0.1$, a dynamical blockade with two windows appears, whereas at $\Delta_s/\omega_m = 0.15$, only a single window is observed [the inset in Fig. 3(b)].

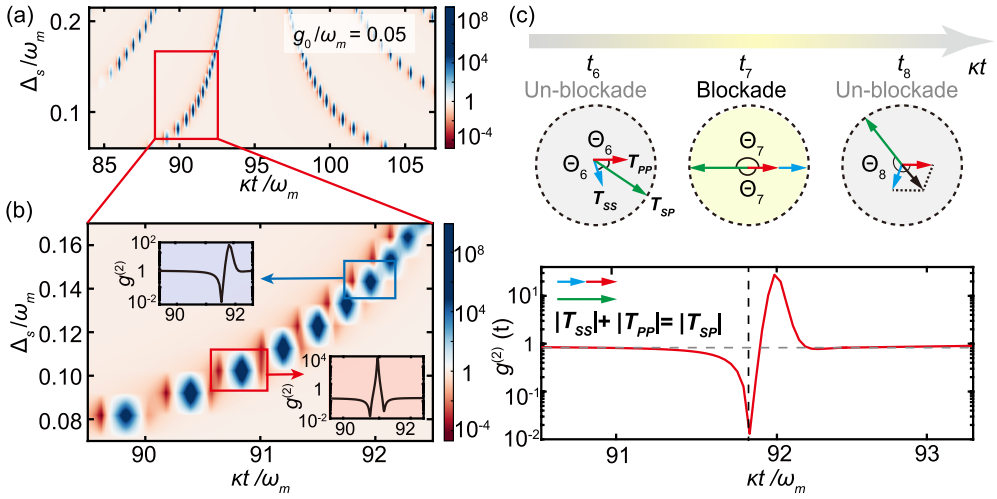

Fig. 3. Switching between single and double windows of OMPB by tuning the detuning. (a) The equal-time second-order correlation function $g^{(2)}(t)$ as a function of $\kappa t/\omega_m$ and detuning Δ_s/ω_m with a coupling rate $g_0/\omega_m = 0.05$. (b) Enlarged view of (a) illustrating the blockade window switch from single to double. The insets show $g^{(2)}(t)$ versus $\kappa t/\omega_m$ for two blockade windows ($\Delta_s/\omega_m = 0.1$) and a single blockade window ($\Delta_s/\omega_m = 0.15$). (c) Diagrams of probability amplitudes for different pathways at $\Delta_s/\omega_m = 0.15$ in polar coordinate spaces at different times. Here, the phase angle is defined as $\Theta_j = \theta + \Delta_s \cdot t_j$ for $j = 6, 7, 8$. Other parameters are the same as in Fig. 2.

Additionally, we plotted the transition amplitudes in polar coordinates for $\Delta_s/\omega_m = 0.15$ over different times and paths, as illustrated in Fig. 3(c). We observe that the relationship between the transition amplitudes for different paths is $|T_{sp}| = |T_{ss}| + |T_{pp}|$, indicating a single optimal interference time and hence a single blockade window within one period. This differs from the condition of dynamical blockade characterized by two blockade windows. Our scheme can control the switching between single and double-blockade windows, maintaining a strong quantum effect even at the single blockade window.

In the following, we illustrate the dependence of the minimum of $g^{(2)}(t)$ on the optomechanical coupling strength g_0. In Fig. 4(a), we show the variation of $g^{(2)}(t)$ with time and coupling strength, and found that by controlling the mechanical cavity coupling strength gradually increased, the photon blockade will gradually enhanced as well. According to Eq. (16), the minimum $g^{(2)}(t)$ is proportional to the coupling strength. The quantum interference is also related with the coupling strength, for example, under weak nonlinearity $g_0/\omega_m = 0.05$, the minimum value of $g^{(2)}(t)$ can reach 10^{-4} [Fig. 4(a)].

The blockade time reflects the stability of the system and is a key consideration in practical experiments, so we define the time window ΔT of photon blockade as a duration of $g^{(2)}(t)<0.95$ [87], as shown in Fig. 4(c). When the coupling strength g_0 takes various values, as shown in Fig. 4(d), the time ratio of non-classical optical fields gradually increases. This means that the

Optics EXPRESS

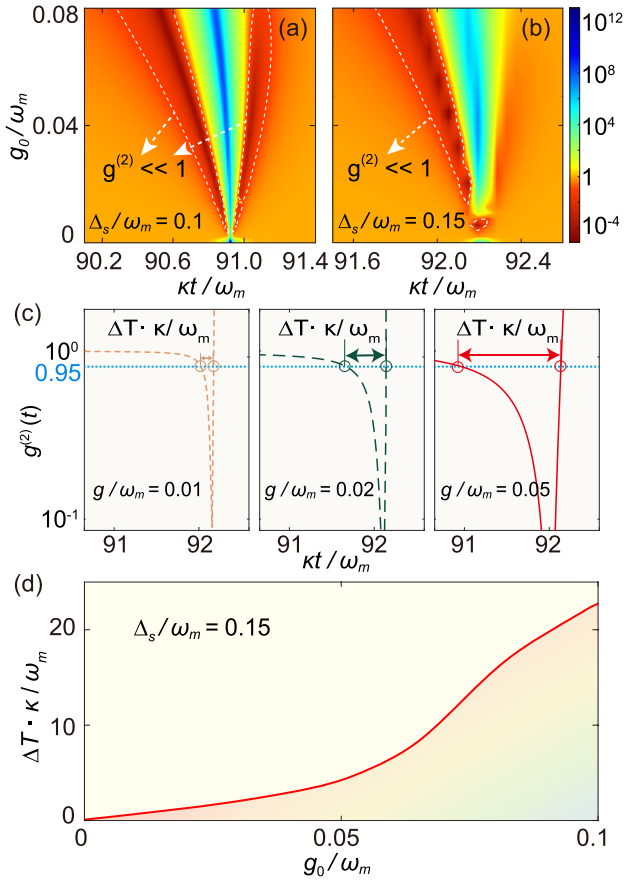

Fig. 4. The influence of coupling strength on OMPB window. (a) The second-order correlation function for two blockade windows and (b) for a single blockade window, both increasing with the coupling rate g_0. The white line indicates the region where $g^{(2)} \ll 1$. (c) Width of the time window ΔT for $g^{(2)}(t)$<0.95 under several weak coupling rates g_0 with $\Delta_s/\omega_m = 0.15$. (d) Dependence of the width of ΔT on the coupling rate g_0. Other parameters are as the same as in Fig. 2.

Optics EXPRESS

time window of photon blockade is affected by the coupling strength. Figures 4(c) and (d) to show that effective photon blockade can be achieved under the weak coupling regime $g_0/\omega_m \sim 0.1$.

Here, we propose how to realize and measure this bi-tone driven OMPB with state-of-the-art techniques and experimentally accessible parameters. The second-order correlation function $g^{(2)}(t)$ is directly accessible via a Hanbury Brown-Twiss setup at the cavity output [95,97–100]. In our scheme, the required bi-tone field is readily generated using a single narrow-linewidth laser and an electro-optic modulator [87]; standard electronic channels control the amplitude ratio ϵ_s/ϵ_p and lock the phase with percent-level precision. For the optomechanical systems [2,51,101–104], the mechanical frequency $\omega_m/2\pi \sim 10^2 - 10^9$ Hz, the the coupling strength $g_0/2\pi \sim 10^{-3} - 10^6$ Hz, the optical dissipation rate $\kappa/2\pi \sim 10^2 - 10^{11}$ Hz, and the mechanical damping rate $\gamma_m/2\pi \sim 10^{-5} - 10^5$ Hz. Therefore, the parameters used in our study, $g_0/\omega_m = 0.05$, $\kappa/\omega_m = 0.15$, $\gamma_m/\omega_m = 0.001$, are within reach of current cavity optomechanical systems.

4. Conclusion

In conclusion, we have proposed to achieve optomechanical dynamical photon blockade effect without requiring the non-realistic condition of strong light-motion coupling, by using two coherent driving fields. We find that by utilizing the destructive quantum interference between different transition paths provided by this bi-tone-driven strategy, full cancellation of the two-photon populations is achievable even with weak optomechanical coupling, which in turn leads to the occurrence of photon blockade in such a system.

Single photons are essential to many quantum technologies. Compared to previous works [71,81–84,92], our scheme eliminates the need for strong optomechanical coupling or precise tuning of intrinsic system parameters, which relies solely on bi-tone coherent driving. Thus this strategy can be further extended to a variety of hybrid quantum systems to realize nonclassical effects, including photon bundles [105–108], optomechanical cat states [109–111], light-motion entanglement [68,112–114], single-photon sources with anharmonic energy spectra [115], and even bi-tone-driven quantum metrology [116]. Moreover, the simplicity and generality of our scheme highlight its potential for realizing single-photon devices across a broad class of optomechanical platforms for quantum information and photonics applications.

Funding. National Natural Science Foundation of China (92365107, 12347136); National Key Research and Development Program of China (2019YFA0308700, 2024YFE0102400); Program for Innovative Talents and Teams in Jiangsu (JSSCTD202138); Postdoctoral Fellowship Program (Grade 247 C) of China Postdoctoral Science Foundation (GZC20231726).

Disclosures. The authors declare no conflicts of interest.

Data availability. No data were generated or analyzed in the presented research.

References

1. S. Barzanjeh, A. Xuereb, S. Gröblacher, *et al.*, "Optomechanics for quantum technologies," Nat. Phys. **18**(1), 15–24 (2022).
2. M. Aspelmeyer, T. J. Kippenberg, and F. Marquardt, "Cavity optomechanics," Rev. Mod. Phys. **86**(4), 1391–1452 (2014).
3. M. Bagheri, M. Poot, M. Li, *et al.*, "Dynamic manipulation of nanomechanical resonators in the high-amplitude regime and non-volatile mechanical memory operation," Nat. Nanotechnol. **6**(11), 726–732 (2011).
4. S. Kolkowitz, A. C. Bleszynski Jayich, Q. P. Unterreithmeier, *et al.*, "Coherent sensing of a mechanical resonator with a single-spin qubit," Science **335**(6076), 1603–1606 (2012).
5. M. Hafezi and P. Rabl, "Optomechanically induced non-reciprocity in microring resonators," Opt. Express **20**(7), 7672–7684 (2012).
6. A. Metelmann and A. A. Clerk, "Nonreciprocal Photon Transmission and Amplification via Reservoir Engineering," Phys. Rev. X **5**(2), 021025 (2015).
7. M.-A. Miri, F. Ruesink, E. Verhagen, *et al.*, "Optical Nonreciprocity Based on Optomechanical Coupling," Phys. Rev. Appl. **7**(6), 064014 (2017).
8. X. Su, J.-S. Tang, and K. Xia, "Nonlinear dissipation-induced photon blockade," Phys. Rev. A **106**(6), 063707 (2022).

Optics EXPRESS

9. N. R. Bernier, L. D. Toth, A. Koottandavida, *et al.*, "Nonreciprocal reconfigurable microwave optomechanical circuit," Nat. Commun. **8**(1), 604 (2017).
10. G. A. Peterson, F. Lecocq, K. Cicak, *et al.*, "Demonstration of Efficient Nonreciprocity in a Microwave Optomechanical Circuit," Phys. Rev. X **7**(3), 031001 (2017).
11. S. Barzanjeh, M. Wulf, M. Peruzzo, *et al.*, "Mechanical on-chip microwave circulator," Nat. Commun. **8**(1), 953 (2017).
12. S. Forstner, S. Prams, J. Knittel, *et al.*, "Cavity Optomechanical Magnetometer," Phys. Rev. Lett. **108**(12), 120801 (2012).
13. J. Hertzberg, T. Rocheleau, T. Ndukum, *et al.*, "Back-action-evading measurements of nanomechanical motion," Nat. Phys. **6**(3), 213–217 (2010).
14. A. G. Krause, M. Winger, T. D. Blasius, *et al.*, "A high-resolution microchip optomechanical accelerometer," Nat. Photonics **6**(11), 768–772 (2012).
15. E. Gavartin, P. Verlot, and T. J. Kippenberg, "A hybrid on-chip optomechanical transducer for ultrasensitive force measurements," Nat. Nanotechnol. **7**(8), 509–514 (2012).
16. W. Zhao, S.-D. Zhang, A. Miranowicz, *et al.*, "Weak-force sensing with squeezed optomechanics," Sci. China: Phys. Mech. Astron. **63**(2), 224211 (2020).
17. S.-D. Zhang, J. Wang, Q. Zhang, *et al.*, "Squeezing-enhanced quantum sensing with quadratic optomechanics," Opt. Quantum **2**(4), 222–229 (2024).
18. J. Wang, Q. Zhang, Y.-F. Jiao, *et al.*, "Quantum advantage of one-way squeezing in weak-force sensing," Appl. Phys. Rev. **11**(3), 031409 (2024).
19. J. Aasi, J. Abadie, B. Abbott, *et al.*, "Enhanced sensitivity of the LIGO gravitational wave detector by using squeezed states of light," Nat. Photonics **7**(8), 613–619 (2013).
20. M. Tse, H. Yu, N. Kijbunchoo, *et al.*, "Quantum-Enhanced Advanced LIGO Detectors in the Era of Gravitational-Wave Astronomy," Phys. Rev. Lett. **123**(23), 231107 (2019).
21. F. Marquardt, J. P. Chen, A. A. Clerk, *et al.*, "Quantum Theory of Cavity-Assisted Sideband Cooling of Mechanical Motion," Phys. Rev. Lett. **99**(9), 093902 (2007).
22. J. M. Dobrindt, I. Wilson-Rae, and T. J. Kippenberg, "Parametric Normal-Mode Splitting in Cavity Optomechanics," Phys. Rev. Lett. **101**(26), 263602 (2008).
23. S. Gröblacher, K. Hammerer, M. R. Vanner, *et al.*, "Observation of strong coupling between a micromechanical resonator and an optical cavity field," Nature **460**(7256), 724–727 (2009).
24. S. Huang and G. S. Agarwal, "Normal-mode splitting in a coupled system of a nanomechanical oscillator and a parametric amplifier cavity," Phys. Rev. A **80**(3), 033807 (2009).
25. I. S. Grudinin, H. Lee, O. Painter, *et al.*, "Phonon Laser Action in a Tunable Two-Level System," Phys. Rev. Lett. **104**(8), 083901 (2010).
26. R. M. Pettit, W. Ge, P. Kumar, *et al.*, "An optical tweezer phonon laser," Nat. Photonics **13**(6), 402–405 (2019).
27. D. L. Chafatinos, A. Kuznetsov, S. Anguiano, *et al.*, "Polariton-driven phonon laser," Nat. Commun. **11**(1), 4552 (2020).
28. T. Kuang, R. Huang, W. Xiong, *et al.*, "Nonlinear multi-frequency phonon lasers with active levitated optomechanics," Nat. Phys. **19**(3), 414–419 (2023).
29. H. Jing, Ş. K. Özdemir, X.-Y. Lü, *et al.*, "$\mathcal{PT}$-Symmetric Phonon Laser," Phys. Rev. Lett. **113**(5), 053604 (2014).
30. J. Zhang, B. Peng, Ş. K. Özdemir, *et al.*, "A phonon laser operating at an exceptional point," Nat. Photonics **12**(8), 479–484 (2018).
31. H. Lü, Ş. K. Özdemir, L.-M. Kuang, *et al.*, "Exceptional Points in Random-Defect Phonon Lasers," Phys. Rev. Appl. **8**(4), 044020 (2017).
32. Y. Jiang, S. Maayani, T. Carmon, *et al.*, "Nonreciprocal Phonon Laser," Phys. Rev. Appl. **10**(6), 064037 (2018).
33. Y.-L. Zhang, C.-L. Zou, C.-S. Yang, *et al.*, "Phase-controlled phonon laser," New J. Phys. **20**(9), 093005 (2018).
34. T.-X. Lu, Y. Wang, K. Xia, *et al.*, "Quantum squeezing induced nonreciprocal phonon laser," Sci. China: Phys. Mech. Astron. **67**(6), 260312 (2024).
35. G. S. Agarwal and S. Huang, "Electromagnetically induced transparency in mechanical effects of light," Phys. Rev. A **81**(4), 041803 (2010).
36. S. Weis, R. Rivière, S. Deléglise, *et al.*, "Optomechanically induced transparency," Science **330**(6010), 1520–1523 (2010).
37. A. H. Safavi-Naeini, T. M. Alegre, J. Chan, *et al.*, "Electromagnetically induced transparency and slow light with optomechanics," Nature **472**(7341), 69–73 (2011).
38. H. Jing, Ş. K. Özdemir, Z. Geng, *et al.*, "Optomechanically-induced transparency in parity-time-symmetric microresonators," Sci. Rep. **5**(1), 9663 (2015).
39. H. Lü, C. Wang, L. Yang, *et al.*, "Optomechanically Induced Transparency at Exceptional Points," Phys. Rev. Appl. **10**(1), 014006 (2018).
40. H. Zhang, F. Saif, Y. Jiao, *et al.*, "Loss-induced transparency in optomechanics," Opt. Express **26**(19), 25199–25210 (2018).
41. M. Peng, H. Zhang, Q. Zhang, *et al.*, "Nonreciprocal slow or fast light in anti-$\mathcal{PT}$-symmetric optomechanics," Phys. Rev. A **107**(3), 033507 (2023).
42. H. Lü, Y. Jiang, Y.-Z. Wang, *et al.*, "Optomechanically induced transparency in a spinning resonator," Photonics Res. **5**(4), 367–371 (2017).

Optics EXPRESS

43. X.-Y. Lü, H. Jing, J.-Y. Ma, *et al.*, "$\mathcal{PT}$-Symmetry-Breaking Chaos in Optomechanics," Phys. Rev. Lett. **114**(25), 253601 (2015).
44. M. Chen, J. Tang, L. Tang, *et al.*, "Photon blockade and single-photon generation with multiple quantum emitters," Phys. Rev. Res. **4**(3), 033083 (2022).
45. H. Jing, Ş. Özdemir, H. Lü, *et al.*, "High-order exceptional points in optomechanics," Sci. Rep. **7**(1), 3386 (2017).
46. V. Peano, C. Brendel, M. Schmidt, *et al.*, "Topological Phases of Sound and Light," Phys. Rev. X **5**(3), 031011 (2015).
47. H. Xu, D. Mason, L. Jiang, *et al.*, "Topological energy transfer in an optomechanical system with exceptional points," Nature **537**(7618), 80–83 (2016).
48. J. Cha, K. W. Kim, and C. Daraio, "Experimental realization of on-chip topological nanoelectromechanical metamaterials," Nature **564**(7735), 229–233 (2018).
49. A. Youssefi, S. Kono, A. Bancora, *et al.*, "Topological lattices realized in superconducting circuit optomechanics," Nature **612**(7941), 666–672 (2022).
50. H. Ren, T. Shah, H. Pfeifer, *et al.*, "Topological phonon transport in an optomechanical system," Nat. Commun. **13**(1), 3476 (2022).
51. J. Chan, T. M. Alegre, A. H. Safavi-Naeini, *et al.*, "Laser cooling of a nanomechanical oscillator into its quantum ground state," Nature **478**(7367), 89–92 (2011).
52. J. D. Teufel, T. Donner, D. Li, *et al.*, "Sideband cooling of micromechanical motion to the quantum ground state," Nature **475**(7356), 359–363 (2011).
53. K. Xia and J. Evers, "Ground state cooling of a nanomechanical resonator in the nonresolved regime via quantum interference," Phys. Rev. Lett. **103**(22), 227203 (2009).
54. K. Xia and J. Evers, "Ground-state cooling of a nanomechanical resonator coupled to two interacting flux qubits," Phys. Rev. B **82**(18), 184532 (2010).
55. A. D. O'Connell, M. Hofheinz, M. Ansmann, *et al.*, "Quantum ground state and single-phonon control of a mechanical resonator," Nature **464**(7289), 697–703 (2010).
56. N. Fiaschi, B. Hensen, A. Wallucks, *et al.*, "Optomechanical quantum teleportation," Nat. Photonics **15**(11), 817–821 (2021).
57. N. Lauk, N. Sinclair, S. Barzanjeh, *et al.*, "Perspectives on quantum transduction," Quantum Sci. Technol. **5**(2), 020501 (2020).
58. A. Clerk, K. Lehnert, P. Bertet, *et al.*, "Hybrid quantum systems with circuit quantum electrodynamics," Nat. Phys. **16**(3), 257–267 (2020).
59. E. E. Wollman, C. Lei, A. Weinstein, *et al.*, "Quantum squeezing of motion in a mechanical resonator," Science **349**(6251), 952–955 (2015).
60. J.-M. Pirkkalainen, E. Damskägg, M. Brandt, *et al.*, "Squeezing of Quantum Noise of Motion in a Micromechanical Resonator," Phys. Rev. Lett. **115**(24), 243601 (2015).
61. F. Lecocq, J. B. Clark, R. W. Simmonds, *et al.*, "Quantum Nondemolition Measurement of a Nonclassical State of a Massive Object," Phys. Rev. X **5**(4), 041037 (2015).
62. S. Barzanjeh, E. Redchenko, M. Peruzzo, *et al.*, "Stationary entangled radiation from micromechanical motion," Nature **570**(7762), 480–483 (2019).
63. S. Hong, R. Riedinger, I. Marinković, *et al.*, "Hanbury Brown and Twiss interferometry of single phonons from an optomechanical resonator," Science **358**(6360), 203–206 (2017).
64. R. Riedinger, A. Wallucks, I. Marinković, *et al.*, "Remote quantum entanglement between two micromechanical oscillators," Nature **556**(7702), 473–477 (2018).
65. C. Ockeloen-Korppi, E. Damskägg, J.-M. Pirkkalainen, *et al.*, "Stabilized entanglement of massive mechanical oscillators," Nature **556**(7702), 478–482 (2018).
66. L. Mercier de Lépinay, C. F. Ockeloen-Korppi, M. J. Woolley, *et al.*, "Quantum mechanics–free subsystem with mechanical oscillators," Science **372**(6542), 625–629 (2021).
67. S. Kotler, G. A. Peterson, E. Shojaee, *et al.*, "Direct observation of deterministic macroscopic entanglement," Science **372**(6542), 622–625 (2021).
68. Y.-F. Jiao, S.-D. Zhang, Y.-L. Zhang, *et al.*, "Nonreciprocal Optomechanical Entanglement against Backscattering Losses," Phys. Rev. Lett. **125**(14), 143605 (2020).
69. V. Macrì, A. Ridolfo, O. Di Stefano, *et al.*, "Nonperturbative Dynamical Casimir Effect in Optomechanical Systems: Vacuum Casimir-Rabi Splittings," Phys. Rev. X **8**(1), 011031 (2018).
70. B. Wang, F. Nori, and Z.-L. Xiang, "Quantum Phase Transitions in Optomechanical Systems," Phys. Rev. Lett. **132**(5), 053601 (2024).
71. P. Rabl, "Photon Blockade Effect in Optomechanical Systems," Phys. Rev. Lett. **107**(6), 063601 (2011).
72. J.-Q. Liao and F. Nori, "Photon blockade in quadratically coupled optomechanical systems," Phys. Rev. A **88**(2), 023853 (2013).
73. R. Huang, A. Miranowicz, J.-Q. Liao, *et al.*, "Nonreciprocal photon blockade," Phys. Rev. Lett. **121**(15), 153601 (2018).
74. C. Zhai, R. Huang, H. Jing, *et al.*, "Mechanical switch of photon blockade and photon-induced tunneling," Opt. Express **27**(20), 27649–27662 (2019).
75. R. Huang, Ş. K. Özdemir, J.-Q. Liao, *et al.*, "Exceptional photon blockade: Engineering photon blockade with chiral exceptional points," Laser Photonics Rev. **16**(7), 2100430 (2022).

Optics EXPRESS

76. Y. Zuo, R. Huang, L.-M. Kuang, *et al.*, "Loss-induced suppression, revival, and switch of photon blockade," Phys. Rev. A **106**(4), 043715 (2022).
77. X.-Y. Lú, W.-M. Zhang, S. Ashhab, *et al.*, "Quantum-criticality-induced strong Kerr nonlinearities in optomechanical systems," Sci. Rep. **3**(1), 2943 (2013).
78. X.-Y. Lü, Y. Wu, J. R. Johansson, *et al.*, "Squeezed Optomechanics with Phase-Matched Amplification and Dissipation," Phys. Rev. Lett. **114**(9), 093602 (2015).
79. M.-A. Lemonde, N. Didier, and A. A. Clerk, "Enhanced nonlinear interactions in quantum optomechanics via mechanical amplification," Nat. Commun. **7**(1), 11338 (2016).
80. F. Zou, L.-B. Fan, J.-F. Huang, *et al.*, "Enhancement of few-photon optomechanical effects with cross-Kerr nonlinearity," Phys. Rev. A **99**(4), 043837 (2019).
81. T. C. H. Liew and V. Savona, "Single Photons from Coupled Quantum Modes," Phys. Rev. Lett. **104**(18), 183601 (2010).
82. M. Bamba, A. Imamoğlu, I. Carusotto, *et al.*, "Origin of strong photon antibunching in weakly nonlinear photonic molecules," Phys. Rev. A **83**(2), 021802 (2011).
83. H. J. Snijders, J. A. Frey, J. Norman, *et al.*, "Observation of the Unconventional Photon Blockade," Phys. Rev. Lett. **121**(4), 043601 (2018).
84. C. Vaneph, A. Morvan, G. Aiello, *et al.*, "Observation of the Unconventional Photon Blockade in the Microwave Domain," Phys. Rev. Lett. **121**(4), 043602 (2018).
85. B. Li, R. Huang, X. Xu, *et al.*, "Nonreciprocal unconventional photon blockade in a spinning optomechanical system," Photonics Res. **7**(6), 630–641 (2019).
86. S. Ghosh and T. C. H. Liew, "Dynamical blockade in a single-mode bosonic system," Phys. Rev. Lett. **123**(1), 013602 (2019).
87. M. Li, Y.-L. Zhang, S.-H. Wu, *et al.*, "Single-Mode Photon Blockade Enhanced by Bi-Tone Drive," Phys. Rev. Lett. **129**(4), 043601 (2022).
88. K. Xia, Y. Niu, C. Li, *et al.*, "Absolute phase control of spectra effects in a two-level medium driven by two-color ultrashort laser pulses," Phys. Lett. A **361**(1-2), 173–177 (2007).
89. D.-W. Liu, Z.-H. Li, S.-L. Chao, *et al.*, "Dynamical switchable quantum nonreciprocity induced by off-resonant chiral two-photon driving," Sci. China Phys. Mech. Astron. **67**(6), 260313 (2024).
90. B. Sarma and A. K. Sarma, "Unconventional photon blockade in three-mode optomechanics," Phys. Rev. A **98**(1), 013826 (2018).
91. J. R. Johansson, P. D. Nation, and F. Nori, "QuTiP 2: A Python framework for the dynamics of open quantum systems," Comput. Phys. Commun. **184**(4), 1234–1240 (2013).
92. H. Flayac and V. Savona, "Unconventional photon blockade," Phys. Rev. A **96**(5), 053810 (2017).
93. D.-Y. Wang, C.-H. Bai, X. Han, *et al.*, "Enhanced photon blockade in an optomechanical system with parametric amplification," Opt. Lett. **45**(9), 2604–2607 (2020).
94. T. Volz, A. Reinhard, M. Winger, *et al.*, "Ultrafast all-optical switching by single photons," Nat. Photonics **6**(9), 605–609 (2012).
95. B. Dayan, A. S. Parkins, T. Aoki, *et al.*, "A photon turnstile dynamically regulated by one atom," Science **319**(5866), 1062–1065 (2008).
96. A. Javadi, M. Söllner, I. Arcari, *et al.*, "Single-photon non-linear optics with a quantum dot in a waveguide," Nat. Commun. **6**(1), 8655 (2015).
97. K. M. Birnbaum, A. Boca, R. Miller, *et al.*, "Photon blockade in an optical cavity with one trapped atom," Nature (London) **436**(7047), 87–90 (2005).
98. C. Hamsen, K. N. Tolazzi, T. Wilk, *et al.*, "Strong coupling between photons of two light fields mediated by one atom," Nat. Phys. **14**(9), 885–889 (2018).
99. K. Hennessy, A. Badolato, M. Winger, *et al.*, "Quantum nature of a strongly coupled single quantum dot–cavity system," Nature (London) **445**(7130), 896–899 (2007).
100. A. Faraon, I. Fushman, D. Englund, *et al.*, "Coherent generation of non-classical light on a chip via photon-induced tunnelling and blockade," Nat. Phys. **4**(11), 859–863 (2008).
101. E. Verhagen, S. Deléglise, S. W. A. Schliesser, *et al.*, "Quantum-coherent coupling of a mechanical oscillator to an optical cavity mode," Nature (London) **482**(7383), 63–67 (2012).
102. F. Brennecke, S. Ritter, T. Donner, *et al.*, "Cavity optomechanics with a bose-einstein condensate," Science **322**(5899), 235–238 (2008).
103. K. W. Murch, K. L. Moore, S. Gupta, *et al.*, "Observation of quantum-measurement backaction with an ultracold atomic gas," Nat. Phys. **4**(7), 561–564 (2008).
104. M. Eichenfield, R. Camacho, J. Chan, *et al.*, "A picogram- and nanometre-scale photonic-crystal optomechanical cavity," Nature (London) **459**(7246), 550–555 (2009).
105. C. S. Muñoz, E. del Valle, A. G. Tudela, *et al.*, "Emitters of n-photon bundles," Nat. Photonics **8**(7), 550–555 (2014).
106. Q. Bin, X.-Y. Lü, F. P. Laussy, *et al.*, "*n*-phonon bundle emission via the stokes process," Phys. Rev. Lett. **124**(5), 053601 (2020).
107. Q. Bin, Y. Wu, and X.-Y. Lü, "Parity-symmetry-protected multiphoton bundle emission," Phys. Rev. Lett. **127**(7), 073602 (2021).
108. F. Zou, Y. Li, and J.-Q. Liao, "Dynamical n-photon bundle emission," New J. Phys. **25**(4), 043027 (2023).

Optics EXPRESS

109. B. D. Hauer, J. Combes, and J. D. Teufel, "Nonlinear sideband cooling to a cat state of motion," Phys. Rev. Lett. **130**(21), 213604 (2023).
110. B. Li, W. Qin, Y.-F. Jiao, *et al.*, "Optomechanical schrödinger cat states in a cavity bose-einstein condensate," Fundam. Res. **3**(1), 15–20 (2023).
111. J.-Q. Liao and L. Tian, "Macroscopic quantum superposition in cavity optomechanics," Phys. Rev. Lett. **116**(16), 163602 (2016).
112. Y.-D. Wang and A. A. Clerk, "Reservoir-engineered entanglement in optomechanical systems," Phys. Rev. Lett. **110**(25), 253601 (2013).
113. J.-X. Liu, J.-Y. Yang, T.-X. Lu, *et al.*, "Phase-controlled robust quantum entanglement of remote mechanical oscillators," Phys. Rev. A **109**(2), 023519 (2024).
114. Y. Li, Y.-F. Jiao, J.-X. Liu, *et al.*, "Vector optomechanical entanglement," Nanophotonics **11**(1), 67–77 (2021).
115. Z. Geng, Y. Chen, Y. Jiang, *et al.*, "Engineering dynamical photon blockade with liouville exceptional points," Opt. Lett. **49**(11), 3026–3029 (2024).
116. L. Pezzè, A. Smerzi, M. K. Oberthaler, *et al.*, "Quantum metrology with nonclassical states of atomic ensembles," Rev. Mod. Phys. **90**(3), 035005 (2018).